Mon. Not. R. Astron. Soc. **000**, 1–11 (2004) Printed 1 November 2018 (MN LATEX style file v2.2)

White dwarf envelopes: further results of a non-local model of convection

M. H. Montgomery[1] & F. Kupka[2,3]
[1]*Institute of Astronomy, University of Cambridge, Madingley Road, Cambridge CB3 0HA, United Kingdom*
[2]*Astronomy Unit, School of Mathematical Sciences, Queen Mary, University of London, Mile End Road, London E1 4NS*
[3]*Max-Planck-Institute for Astrophysics, Karl-Schwarzschild-Str. 1, 85741 Garching, Germany*

arXiv:astro-ph/0401489v1 23 Jan 2004

Accepted 2004 January 22

ABSTRACT

We present results of a fully non-local model of convection for white dwarf envelopes. We show that this model is able to reproduce the results of numerical simulations for convective efficiencies ranging from very inefficient to moderately efficient; this agreement is made more impressive given that *no closure parameters have been adjusted* in going from the previously reported case of A-stars to the present case of white dwarfs; for comparison, in order to match the peak convective flux found in numerical simulations for both the white dwarf envelopes discussed in this paper and the A-star envelopes discussed in our previous work requires changing the mixing length parameter of commonly used local models by a factor of 4. We also examine in detail the overshooting at the base of the convection zone, both in terms of the convective flux and in terms of the velocity field: we find that the flux overshoots by $\sim 1.25 H_P$ and the velocity by $\sim 2.5 H_P$. Due to the large amount of overshooting found at the base of the convection zone the new model predicts the mixed region of white dwarf envelopes to contain at least 10 times more mass than local mixing length theory (MLT) models having similar photospheric temperature structures. This result is consistent with the upper limit given by numerical simulations which predict an even larger amount of mass to be mixed by convective overshooting. Finally, we attempt to parametrise some of our results in terms of local MLT-based models, insofar as is possible given the limitations of MLT.

Key words: convection, stars: white dwarfs, atmospheres, interiors

1 INTRODUCTION

Understanding white dwarf stars is crucial for many areas of astrophysics. First, their masses can be used to place constraints on mass loss in the post-Main Sequence phase and hence on the initial-final mass relation (Weidemann 2000). Second, their temperatures can be used to derive ages, either individually, for clusters, or for the local Galactic disk (e.g. Winget et al. 1987; Wood 1992). Complementary to this, white dwarfs are observed to pulsate in specific temperature ranges, and these pulsations allow us to probe and constrain the interior structure of these stars (Winget 1998). Through their pulsations, we can use asteroseismology to examine various physical processes such as nuclear reaction rates (Metcalfe 2003), chemical diffusion (Montgomery et al. 2001), crystallisation (Winget et al. 1997; Montgomery & Winget 1999), and neutrino emission (O'Brien et al. 1998).

In addition, these pulsations are most likely driven through their interaction with the surface convection zone in these stars (Brickhill 1991a; Wu 1997; Goldreich & Wu 1999), meaning that the onset of pulsations (in terms of $T_{\rm eff}$) is linked with the convection zone reaching a certain depth. In many cases the observed amplitudes imply that the depth and structure of these convection zones should vary appreciably (by a factor of several in mass) during a pulsational cycle, and this is thought to be the origin of the dominant nonlinearities in many of the observed lightcurves (Brickhill 1992b; Wu 2001). Given the simplification afforded by the separation of the convective turnover timescale (~ 1 s) and the pulsation timescale (~ 100 s), it is possible to use the pulsations themselves to sample and constrain the convection zones of these stars (Ising & Koester 2001, Montgomery, in preparation). Consequently, other than the well-studied convection zone of the Sun, white dwarfs may offer the best chance for testing theories of stellar convection.

In this paper, we apply the Reynolds stress model formalism for convection (see Kupka & Montgomery 2002) to envelope models of both DA (hydrogen) and DB (helium) white dwarfs. As was the case for convection in A-stars, this problem is made easier numerically by the fact that the white dwarf models we consider have relatively thin surface convection zones, and hence shorter thermal relaxation timescales. As a consequence, we have treated models in which convection is not the dominant form of energy transport, i.e.,

© 2004 RAS

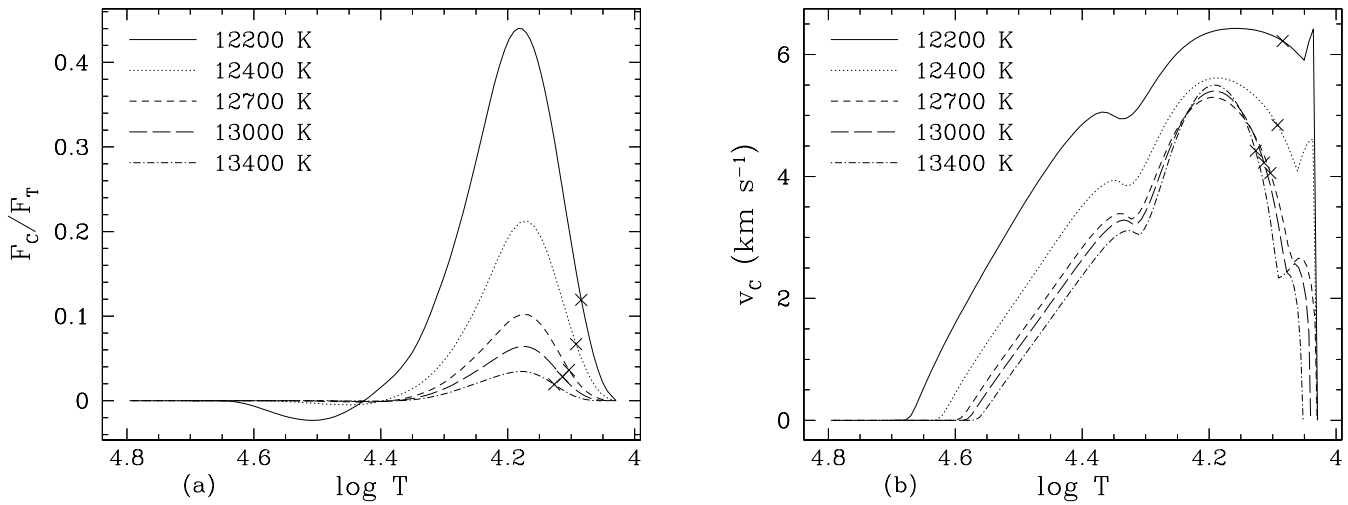

Figure 1. (a) The fraction of the flux carried by convection for five DA white dwarf models with the indicated effective temperatures, where we have taken $\log T$ as our radial variable; $\log g = 8.0$ and $X = 1.00$ ($Z = 0.00$) for all models. The cross on each curve near $\log T \sim 4.1$ shows the location where $\tau = 2/3$ for each model. As expected, convection becomes more dominant with decreasing $T_{\rm eff}$. (b) The same as (a) but for the rms of the vertical component of the convective velocity.

$F_C/F_T \lesssim 0.5$; in this regime, convection is much more sensitive to details in the modelling.

In the sections which follow, we give a brief outline of the physics and the numerical procedure used to compute our envelope models. Results are then presented for models of DA and DB white dwarfs, as a function of $T_{\rm eff}$. Finally, where possible we compare our results to those of numerical simulations and to models used for fitting white dwarf spectra. We show that our calculations qualitatively follow the simulations, especially in terms of the convective flux, and that the photospheric temperature structure of our models is similar to that of previous investigations.

2 DESCRIPTION OF MODEL

The convection model used here is an extension of the Canuto & Dubovikov (1998, hereafter CD98) model which requires the solution of five differential equations of first order in time and second order in space for the hydrodynamic moments K, $\overline{\theta^2}$, $J = \overline{w\theta} = F_C/(\rho c_p)$, $\overline{w^2}$, and ϵ, and of an additional equation for the time evolution of T (cf. equations (1)–(5) and (8) in Kupka 1999); here and throughout this paper, K is the turbulent kinetic energy, θ and w are the temperature and velocity fluctuations, respectively, and ϵ is the turbulent kinetic energy dissipation rate. This system is completed by an equation for the total pressure ('hydrostatic equilibrium' including turbulent pressure, equation (7) in Kupka 1999b) and for the mass ('conservation of mass'). We solve this set of differential equations on an unequally spaced mass grid, with the zoning chosen so as to resolve the gradients in the various quantities. The model equations were derived in a series of papers by Canuto (1992, 1993), CD98, and Canuto et al. (2001). Compressibility effects are taken into account following Canuto (1993). The adoption and solution of these equations for stellar envelopes is described in Kupka & Montgomery (2002), and it is this model which we apply here as well. The closure parameters for correlations such as $\overline{\theta\,\partial p'/\partial x_j}$, i.e. between fluctuations of the temperature and the pressure gradient, which appear in the nonlocal model, have been taken over from the previous paper (see Kupka & Montgomery 2002). We note here that no mixing length is used in this model due to a separate evolution equation for the turbulent kinetic energy dissipation rate ϵ.

For our calculations, we have used a Prandtl number of 10^{-6} as a typical value for the outer part of white dwarf envelopes; values 2 orders of magnitude smaller than this produce essentially identical results. We note that values 2 orders of magnitude *larger* (i.e., 10^{-4}) can alter our results for the hottest models at up to the $\sim$10% level. For the constitutive physics, we use the equation of state and opacity data from the OPAL project (Rogers et al. 1996; Iglesias & Rogers 1996). Since we are treating white dwarfs with pure or nearly pure surface layers, we have taken the metallicity to be zero ($Z = 0.0$), with $X = 1.0$ for the DA (hydrogen spectrum) white dwarfs and $Y = 1.0$ for the DB (helium spectrum) white dwarfs.

While the convection zones we have treated here and in Kupka & Montgomery (2002) are relatively thin surface convection zones, we have solved the full equations for spherical geometry. For upper (outer) boundary conditions, we fix the temperature, gravity, and stellar radius to be equal to those obtained from an envelope model assuming local (MLT) convection, which itself has a given $T_{\rm eff}$, $\log g$, and $R_\star$; thus, both the location of the model in the H-R diagram and its mass are specified (these may be taken either from a self-consistent stellar model or freely specified). We mention that the outer photospheres of these envelope models are completely radiative, so the use of MLT in these models leaves no direct imprint on our subsequent solutions, with the exception of the value derived for the stellar radius, which is slightly affected. At the lower boundary, we assume a constant input luminosity $L_\star$ equal to the luminosity at the stellar surface. The complete system is then integrated in time (currently by a semi-implicit method) until a stationary, thermally relaxed state is found. The mass shells can be re-zoned to a different relative size to resolve, e.g. steep temperature gradients that may appear and/or disappear during convergence. The radiative envelope below the convection zone may then be obtained from a simple downward integration.

Table 1. Convection zone parameters of DA white dwarf models obtained with the non-local model. The overshooting (OV) is defined as the distance in pressure scale heights from the minimum of F_C/F_T to the point where $|F_C/F_T| \sim 10^{-6}$ (similar to L_t in Zahn 1991). OV[mix] is the velocity overshooting; it is defined as the distance from the base of the formally unstable convective region ($\nabla \sim \nabla_{ad}$) to the point where a linear extrapolation of the velocity vanishes (see Fig. 2). Finally, α_{eff} is the value of α for the given mixing length theory (either ML1 or ML2) required to reproduce the peak flux in the convection zone.

T_{eff} (K)	$\log g$	$\log(M_{CZ}/M_\star)$	$(F_C/F_T)_{max}$	OV (in H_p)	$(v_C)_{max}$ (km s^{-1})	$(v_C)_{\tau=2/3}$ (km s^{-1})	OV[mix] (in H_p)	$(p_{turb}/p_{tot})_{max}$	$(p_{turb}/p_{tot})_{\tau=2/3}$	α_{eff} (ML1)	α_{eff} (ML2)
12200	8.00	-14.72	0.4402	1.41	6.43	6.22	2.75	0.290	0.242	1.66	0.65
12400	8.00	-14.93	0.2124	1.37	5.61	4.84	2.45	0.172	0.155	1.57	0.64
12700	8.00	-15.07	0.1020	1.24	5.30	4.05	2.22	0.125	0.106	1.73	0.72
13000	8.00	-15.14	0.0642	1.21	5.40	4.22	2.19	0.125	0.107	2.04	0.85
13400	8.00	-15.22	0.0346	1.14	5.50	4.41	2.15	0.125	0.106	2.53	1.06
12700	8.30	-15.28	0.3414	1.29	5.58	4.98	2.50	0.184	0.161	1.54	0.62
12700	7.70	-14.70	0.0473	1.23	5.88	4.91	2.29	0.152	0.141	2.30	0.96

3 RESULTS

In the following sections, we report results for DA (hydrogen) white dwarfs and DB (helium) white dwarfs. For most of our calculations we have used the canonical value of the white dwarf surface gravity of $\log g = 8.0$, which corresponds to a stellar mass of $\sim 0.6 M_\odot$, although we also present selected results for $\log g = 7.7$ and 8.3.

The temperatures we have explored in these models range from high temperatures in which convection is very inefficient to cooler temperatures for which the convection becomes deeper although not yet adiabatic. Since convection in the DA's is driven by H I partial ionisation and in the DB's mainly by He II partial ionisation, the temperatures of the DB models are much higher; for our DA models, we have chosen temperatures in the range 12,200–13,400 K, and for the DB models 28,000–35,000 K. Observationally, these temperatures approximately correspond to the onset of pulsations in these stars, the so-called 'blue edge' of the pulsational instability strip, which is $\sim$12,500 K for the DA's (Bergeron et al. 1995) and $\sim$28,000 K for the DB's (Beauchamp et al. 1999). These temperatures can be explained either in terms of linear instability due to convective driving (Brickhill 1991a; Goldreich & Wu 1999) or the traditional κ-γ driving mechanism (Winget et al. 1982; Winget 1982). Thus, the *nature* of convection in these stars has a large impact on the properties of the pulsations.

3.1 DA models

For the DA's, we have considered temperatures between 12,200 K and 13,400 K; Fig. 1 shows our central results. First, the models are all strongly convective in the photosphere, with the convective flux being a substantial fraction of the maximum value in the H I convection zone. Second, we see that the photospheric velocities are even larger, attaining values at least as large as 75% of their maximum values within the convection zone. Far out in the photospheres of these models (the crosses indicate the point at which $\tau = 2/3$), we see that the models do become radiative, justifying our use of fully radiative outer boundary conditions. We note that the wiggles near $\log T \sim 4.35$ and 4.07 in the velocity field are due to terms in the equations for third order moments, which represent non-local transport, and whose functional form depends on the sign of N^2 (the square of the Brunt-Väisälä frequency); a smoother model for these terms would remove this feature from the velocities.[1] The actual velocity distribution in transition regions is expected to be smooth, and is found to be so in numerical simulations. We also have to emphasise that the $\log T$ scale does not properly resolve the upper and mid photosphere, hence the apparently very steep drop of velocity at the surface. Comparisons with the convective flux displayed in Fig. 1a and the kinetic energy flux shown in Fig. 3 below indicate what a plot as a function of logarithmic optical depth ($\log \tau_{ross}$) reveals more clearly: a steady and by no means abrupt decay towards zero. Moving the upper boundary further outwards by two orders of magnitude on the optical depth scale would not be noticed in Fig. 1b, as the photospheric temperature has already reached a constant value there due to the underlying approximation of grey radiative transfer.

In Table 1, we give a summary of our results for these DA models. For each model, we give the maximum value of the convective flux, $(F_C/F_T)_{max}$, the overshooting in pressure scale heights of the flux, OV, and the velocity, OV[mix], and the maximum and photospheric values of the vertical component of the convective velocity and the turbulent pressure, v_C and p_{turb}/p_{tot}, respectively. We also give $\log(M_{CZ}/M_\star)$, where M_{CZ} is the total mass of the convection zone, defined as the region which is mixed (including velocity overshooting). Finally, we list values of α_{eff}, which is the value of α which a given MLT model requires in order to reproduce the maximum convective flux. The columns labelled 'ML1' and 'ML2' denote the values obtained using two different versions of MLT, by Böhm-Vitense (1958) and Böhm & Cassinelli (1971), respectively. These versions of MLT will be discussed further in Section 4.

Over the temperature range of the models, we see that for ML1 convection that α_{eff} lies roughly in the range 1.5–2.5; clearly, a local MLT using a single value of α would be unable to reproduce these results. At any rate, this range of values is consistent with those found by Ludwig et al. (1994) in comparison with numerical simulations, and is also consistent with the model atmosphere fits of Koester et al. (1994). In Section 4, we make a more systematic comparison with MLT models (in terms of both ML1 and ML2), taking into account the photospheric temperature structure of the models.

[1] For instance, the non-Gaussian closures recently suggested by Gryanik & Hartmann (2002) should not produce such a feature. Their new model promises a more realistic approach to third and fourth order moments in Reynolds stress models, but requires the solution of additional differential equations.

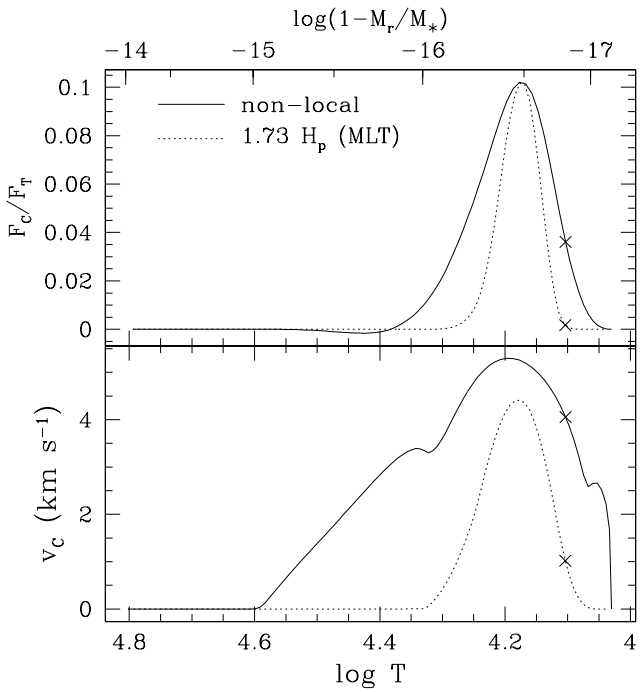

Figure 2. A comparison of the convective fluxes (upper panel) and velocities (lower panel) of the non-local model and of an MLT model ($l = 1.73H_P$), for $T_{\rm eff}$ = 12,700 K. We see that the MLT model cannot simultaneously match the height and width of the convective flux. In addition, the velocity field of the MLT model does not extend as far out into either the photosphere or downward into the envelope as that of the non-local model. Along the top axis we have indicated the depth in terms of the envelope mass $\log(1-M_r/M_\star)$, so that we can see the relative amounts of mass in the formally unstable and overshooting regions.

In Fig. 2, we make a detailed comparison between the flux and velocity structure of our $T_{\rm eff}$ = 12,700 K envelope model with that obtained using the standard MLT prescription for convection. There are at least four aspects of our convection zone solutions which we might wish to compare to MLT: the peak flux and its overshooting depth (i.e. the convectively mixed region), and the peak velocity and *its* overshooting depth. Given the inadequacies of a local MLT, however, it is only possible to fit one of these quantities at a time. Thus, we have adjusted the mixing-length parameter α so that the two models have the same maximum flux; this is achieved for a value of $\alpha = 1.73H_P$. In terms of the convective flux, we see that the non-local model predicts a wider convective region with overshooting extending down to $\log T \sim 4.53$, as compared to the local MLT model, which has its base at $\log T \sim 4.3$. Significantly, the non-local model also predicts a much larger value for the photospheric flux. In terms of the convective velocities, the differences are even larger. The non-local model predicts velocities 50% larger than the local model, and due to overshooting, these velocities also extend much deeper, down to $\log T \sim 4.6$, as compared to $\log T \sim 4.33$ for the local model. Thus, we find that the mass of material 'stirred' by the convection zone is an order of magnitude larger than that which is formally unstable according to a local stability criterion. Among other things, this can have consequences for the diffusion of elements in white dwarf envelopes, as was pointed out by Freytag (1995) and Freytag et al. (1996), who, in addition, found an even larger amount of material stirred below the convection zone in their numerical simulations of DA envelopes (see also Section 5).

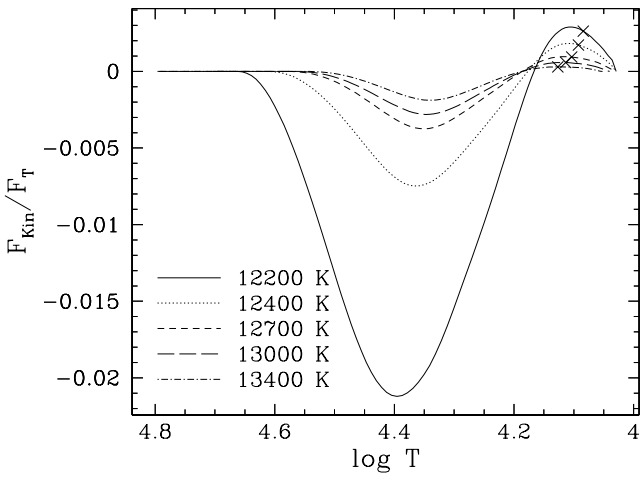

Figure 3. The kinetic energy flux as a function of $\log T$, for the five different models shown in Fig. 1. As expected, the cooler models have larger fluxes. Most significantly, however, these numbers show that $|F_{\rm kin}|$ is essentially negligible for the models we have examined.

3.2 Kinetic energy flux and non-locality

In Fig. 3 we plot the kinetic energy flux for the five different models shown in Fig. 1. Besides the fact that the cooler models have larger fluxes, which is to be expected, we see from the magnitudes of these fluxes that $F_{\rm kin}$ is essentially negligible for the models we have examined. Taking this result at face value, we are thus in a different regime from that of the Sun, in which $|F_{\rm kin}/F_{\rm T}|$ may be as large as 20 per cent (cf. Stein & Nordlund 1998; Kim & Chan 1998). Although a positive $F_{\rm kin}$ in the photosphere indicates that the skewness of spectral lines (and their NLTE cores) produced in this region should also be positive (CD98, cf. the discussion in Kupka & Montgomery 2002), the small magnitude of $F_{\rm kin}$ means that this effect will be small and probably difficult to measure. In the future, it will hopefully be possible to make observational tests of these predictions.

Although the kinetic energy flux in these models appears to be small, this transport of kinetic energy may lead to an equilibrium state having large velocity fields outside of the formally convective regions, provided that the local dissipation rate of kinetic energy is small enough. For instance, in Fig. 2 we see that both below ($\log T \gtrsim 4.4$) and above ($\log T \lesssim 4.05$) the formally convective region there is significant overshooting of the velocities. This can be understood from Fig. 3 since $F_{\rm kin}$ is positive at the top of the formally convective region ($\log T \sim 4.1$), indicating that kinetic energy is being transported outward, while $F_{\rm kin}$ is negative at the bottom of the formally convective region ($\log T \sim 4.4$), indicating that kinetic energy is being transported inward. This velocity overshooting is an essential feature of these models, and is an effect which cannot be captured using local MLT-type models (see Fig. 2 above).

Moreover, even in the formally unstable part of the convection zone, where $F_{\rm kin}$ is small in magnitude compared to $F_{\rm conv}$ (around $\log T \lesssim 4.2$, i.e. where the largest velocities occur), non-local effects remain important. The reason for this result is that in the governing equation for the velocity field in the non-local model, the third order moment directly related to $F_{\rm kin}$, $\overline{q^2 w} = 2F_{\rm kin}/\rho$, appears under a divergence (eq. 1 in Kupka 1999, eqs. 19a, 36a, and 51a in CD98). Thus, the rapid variation of $\overline{q^2 w}$ can cause its divergence to be large even if the third order moments themselves are small

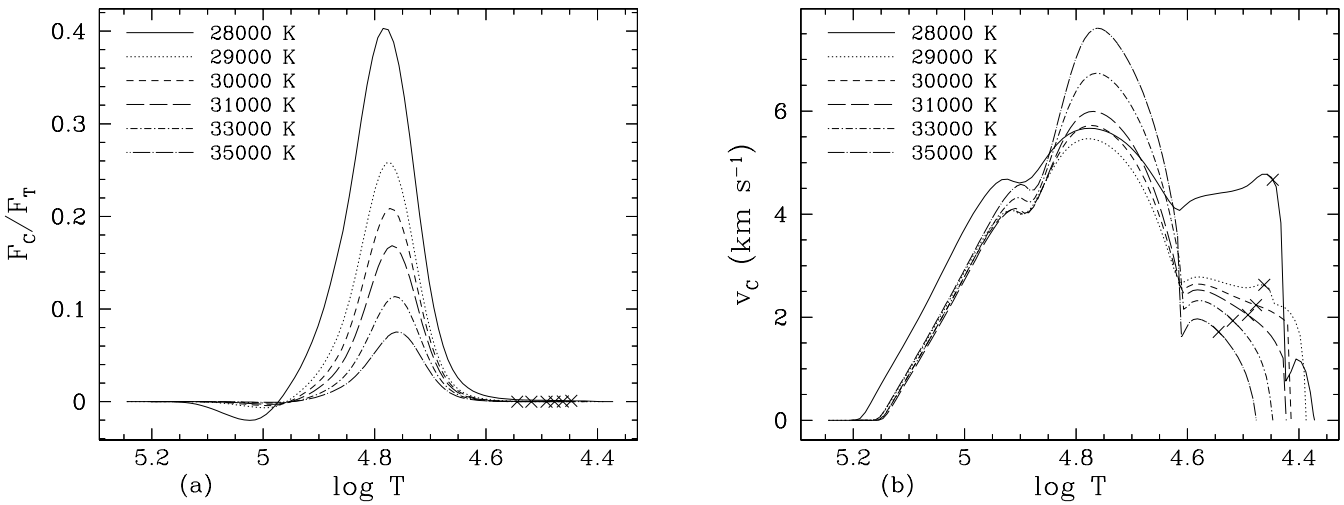

Figure 4. (a) The fraction of the flux carried by convection for six DB white dwarf models with the indicated effective temperatures, as a function of $\log T$; $\log g = 8.0$ and $Y = 1.00$ ($Z = 0.00$) for all models. The crosses in the range of $\log T \sim 4.45$–4.55 show the respective locations of the photospheres ($\tau = 2/3$) of the different models. As expected, convection becomes more efficient with decreasing $T_{\rm eff}$. (b) The same as (a) but for the rms of the vertical component of the convective velocities.

Table 2. The same as Table 1, but for DB white dwarf models.

$T_{\rm eff}$ (K)	$\log g$	$\log(M_{\rm CZ}/M_\star)$	$(F_{\rm C}/F_{\rm T})_{\rm max}$	OV (in H_p)	$(v_{\rm C})_{\rm max}$ (km s^{-1})	$(v_{\rm C})_{\tau=2/3}$ (km s^{-1})	OV[mix] (in H_p)	$(p_{\rm turb}/p_{\rm tot})_{\rm max}$	$(p_{\rm turb}/p_{\rm tot})_{\tau=2/3}$	$\alpha_{\rm eff}$ (ML1)	(ML2)
28000	8.00	-13.28	0.4030	1.33	5.67	4.67	2.53	0.168	0.166	1.14	0.45
29000	8.00	-13.42	0.2577	1.32	5.46	2.62	2.36	0.102	0.057	1.07	0.43
30000	8.00	-13.48	0.2086	1.28	5.72	2.24	2.36	0.111	0.040	1.12	0.45
31000	8.00	-13.51	0.1683	1.29	5.99	2.04	2.36	0.120	0.032	1.16	0.48
33000	8.00	-13.55	0.1136	1.31	6.73	1.93	2.47	0.147	0.027	1.28	0.53
35000	8.00	-13.58	0.0751	1.34	7.60	1.71	2.56	0.177	0.020	1.42	0.59
33000	8.30	-13.96	0.1696	1.31	6.03	2.18	2.41	0.120	0.034	1.20	0.49
33000	7.70	-13.12	0.0736	1.30	7.69	1.51	2.56	0.182	0.016	1.39	0.58

(e.g. as compared to the convective flux). This divergence couples the velocity field with the vertical structure of the model in an interesting manner: fluid elements having differing degrees of partial ionisation are transported to and from neighbouring layers. The ionisation and recombination work and the ionisation energy contained in the gas change the nature of the flow. They hence play an important role in the non-local nature of convection driven by ionisation zones (for the related case of numerical simulations of solar granulation see Rast et al. 1993).

As a consequence, for models of both 'early' white dwarfs and early A-stars we find that their convection zones can be inefficient in the sense of having small convective and kinetic energy fluxes while still having quite large velocity fields, as seen in Fig. 1, and that such large velocities can have significant observational and theoretical consequences. For A-stars, the studies of line profiles discussed in Landstreet (1998) provide a strong observational indication for large velocity fields with a large asymmetry between up- and downflows in these objects. Although such observational indicators are not yet available for white dwarfs, the similarity of non-local models for both A-stars and white dwarfs, which is supported independently by the numerical simulations of Freytag (1995, see also Section 5), suggests that white dwarf envelopes can have significant convective velocities despite having a nearly radiative temperature structure. Thus, the non-local effects, far from being unimportant, manifest themselves in relatively large convective velocities, which in turn can affect the formation and shape of spectral lines in the atmosphere, the diffusion/gravitational settling of elements in the envelope, as well as the way in which any pulsations present in the star interact with the convection zone.

3.3 DB models

For the DB's, we have calculated models with temperatures between 28,000 K and 35,000 K. The analogous results to the DA case are given in Fig. 4 and in Table 2. Besides the general trend that convection becomes more efficient as the temperature decreases, we see that these results are actually quite similar to what we found for the DA's. For instance, the maximum convective velocities of both are in the range 5–6 km/s, their flux overshooting is $\sim 1.25\ H_P$, and their velocity overshooting is $\sim 2.5\ H_P$. One difference between the DA and DB models is the remarkable increase in the photospheric velocity seen in Fig.4b for the coolest model (28,000 K). This is caused by additional driving provided by the partial ionisation of He I. At such low optical depths ($\tau \sim 2/3$) this ionisation zone cannot alter the energy transport, but interestingly, at least within the context of the present, non-local model, it is able to leave a very clear feature in the photospheric surface velocity

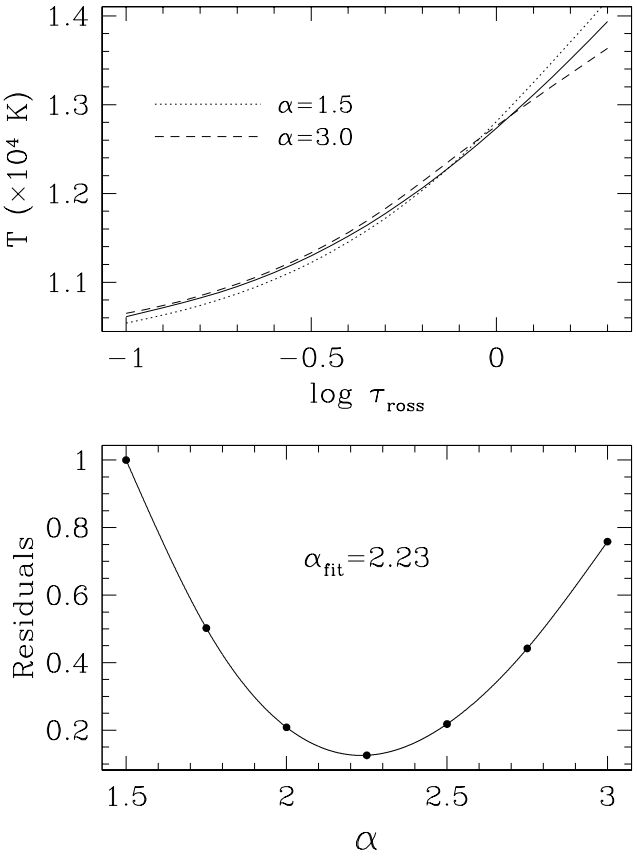

Figure 5. Upper panel: The temperature structure of the photosphere of the $T_{\rm eff}$=12,200 K, $\log g$=8.0 model as a function of optical depth of the non-local model (solid curve) compared to that of local MLT models (ML1) having α = 1.5 (dotted curve) and α = 3.0 (dashed curve). Lower panel: The residuals from a least squares fit as a function of α over this range. The best fit is achieved for α =2.23; for ML2, we find α =0.89.

field. For higher effective temperatures, this ionisation zone moves to even smaller optical depths and its influence on convection vanishes completely.

The other principal differences between the DA and DB models turn out to be in the depth of their convection zones and in their convective efficiencies, as parametrised by $\alpha_{\rm eff}$: the DB's have systematically lower values of $\alpha_{\rm eff}$, and for a given convective flux the DB's have convection zones which are an order of magnitude more massive than those of the DA's. As it turns out, these two results are consistent with each other. Since the He II convection zone is deeper than the H I zone, the MLT eddies contain denser material which has a higher heat capacity and is optically thick, allowing them to transport the same fraction of the total flux with a smaller value of α, i.e., more efficiently.

4 COMPARISON WITH MLT

There are many different ways in which a comparison between the Reynolds stress model and local MLT can be made. In Section 3, we chose to match the maximum of the convective flux in the two models. Since the maxima occur at large optical depths, we are in some sense matching the models in a 'deep' region. Alternatively, we could choose to do the comparison in the photosphere, since this has relevance for model atmosphere fits. In this section, we compare the temperature structure of the photospheres of the local and non-local models; a comparison of the velocity fields is not informative since the local models produce convection zones which are always too narrow for a given convective flux. In addition, the velocity fields used in model atmosphere fits are not usually derived from an underlying convection model but are treated as a free parameter ('microturbulence'), whereas the temperature profiles used in the fits *are* computed using a model of the convection.

Since the temperature structure is most dependent on the convective prescription for models with the largest photospheric convective fluxes, we choose our lowest temperature models for the comparisons. In Fig. 5 we show the results of such a fitting procedure for our $T_{\rm eff}$=12,200 K, $\log g$=8.0 DA model. In the upper panel we plot the temperature as a function of optical depth. We see that the non-local model (solid curve) is bracketed by the local MLT models (ML1) having α = 1.5 (dotted curve) and α = 3.0 (dashed curve). In the lower panel, we plot the results of a least squares fit of the MLT profiles to the non-local profile, as a function of α. The best fit is achieved for a value of α = 2.23. This is in broad agreement with Koester et al. (1994), who find that α = 2.0 yields model spectra which are in reasonable agreement with the observations. In addition, Ludwig et al. (1994) found that the temperature structure of their $T_{\rm eff}$=12,600 K hydrodynamic model could be approximated with values of α between 1 and 2. For *our* $T_{\rm eff}$=12,600 K model, we find it to be bracketed by α = 1.0 and 2.5 models, with a best fit value of α = 1.86, which is consistent with their result.

Many of the current model atmosphere fits for white dwarfs are based on a version of MLT in which radiative energy losses are somewhat suppressed (Böhm & Cassinelli 1971); this version, which is more efficient than ML1 for a given value of α, is often referred to as ML2 (e.g. Tassoul et al. 1990; Ludwig et al. 1999). For our $T_{\rm eff}$=12,200 K model, we find that it is best fit with a value of α = 0.89. For our $T_{\rm eff}$=12,600 K model, we find that the best fit value of α is 0.73. This is in good agreement with Bergeron et al. (1995), who found that their optical spectra of ZZ Ceti's could be well fit by ML2/α = 1.0 models, but that best fits to both the UV and optical spectra were obtained with ML2/α = 0.6, which is the value they adopted for their subsequent analysis.

For our DB models, we are unable to do such fits of the photospheric convective efficiency since the models have so little convection in the photosphere. Thus, the only results comparing our models with local MLT models are the ones already given in Table 2.

5 COMPARISON WITH NUMERICAL SIMULATIONS

In Table 3, we compare the results of our DA models to those from the 2D simulations of Freytag (1995). This comparison is not completely fair due to the fact that different equations of state have been used. Even so, we see that the agreement in terms of the maximum convective fluxes is actually quite good, although the photospheric fluxes do not agree as well. In addition, both the maximum and photospheric values of our vertical convective velocities (v_C) are systematically higher than his by a sizeable margin. At the present, we do not know if this signals an incompleteness in the Reynolds stress model or an inadequacy in the 2D calculations, or both. For instance, Asplund et al. (2000) found that while 2D simulations in the Sun did reasonably well at reproducing the temperature structure of the 3D simulations (and therefore the convective fluxes), the 2D simulations systematically underestimated the magnitude of the convective velocities by 10–20%. In addition, the viscosity used for

Table 3. Comparison of Reynolds stress model results to the numerical simulations of Freytag (1995); all models have $\log g$=8.0. We have used $v_{\rm C}$ and $v_{\rm h}$ to denote the vertical and horizontal rms convective velocities, respectively. Columns labelled RS are the Reynolds stress results, and columns labelled F are the results of Freytag's numerical simulations.

$T_{\rm eff}$ (K)	$(F_{\rm C}/F_{\rm T})_{\rm max}$		$(F_{\rm C}/F_{\rm T})_{\tau=2/3}$		$(v_{\rm C})_{\rm max}$ (km s^{-1})		$(v_{\rm C})_{\tau=2/3}$ (km s^{-1})		$(v_{\rm h})_{\rm max}$ (km s^{-1})		$(v_{\rm h})_{\tau=2/3}$ (km s^{-1})	
	RS	F	RS	F	RS	F	RS	F	RS	F	RS	F
12200	0.440	0.385	0.119	0.036	6.43	3.95	6.22	1.95	6.95	6.38	5.42	6.26
12600	0.126	0.182	0.042	0.043	5.33	3.31	4.16	2.22	4.31	6.01	3.53	5.80
13000	0.064	0.063	0.036	0.020	5.40	2.63	4.22	1.86	4.34	4.14	3.53	3.95
13400	0.035	0.008	0.019	0.006	5.50	1.39	4.41	1.14	4.42	2.23	3.66	1.72

the 2D the simulations may also lead to a reduction of the velocities. Conversely, it is possible that some of the closures in our implementation of the Reynolds stress model may be responsible for this discrepancy (e.g. see Fig. 5 of Kupka 2003). Finally, perhaps surprisingly, we note that the discrepancy between our models is smaller for the horizontal component of the convective velocity, $v_{\rm h}$, than it is for the vertical component.

An interesting question concerns how the velocity field decays beneath the convection zone. Freytag (1995) and Freytag et al. (1996) claim both numerical and theoretical evidence for an exponential decay with depth of the turbulent velocity field; their position is given some support by Ludwig (2003) for the case of overshooting into stellar atmospheres, although he does not find this to be the case for all the models examined. Our equations, on the other hand, lead both analytically and numerically to an approximately linear decay of the velocity field with depth. We claim that the correct behaviour at the base of a convection zone is not yet known, since the way in which one filters out the travelling waves from the truly convective fluid motions has an important effect on the velocity field inferred from the hydrodynamical simulations (Ludwig 2003). Waves, on the other hand, are much less efficient in mixing a fluid than a network of drafts and plumes associated with a 'genuine' convective velocity field. The resolution of this problem has an important bearing on our understanding of diffusion in white dwarf envelopes, since the depth to which convective fluid motions penetrate can greatly affect the diffusion of chemical elements.

Finally, we mention a technical point concerning the Reynolds stress model, which we examine in detail in an appendix. The formalism of Canuto & Dubovikov (1998), which we employ, implicitly assumes for the purpose of statistical averaging that the equation of state is that of an ideal gas. This means that thermodynamic quantities are held constant during averaging, i.e., $\overline{c_P w\theta}$ is replaced by $c_P \overline{w\theta}$.[2] This is not strictly valid since convection zones usually coincide with regions which are partially ionised, so that c_P (and other thermodynamic quantities) are not constants but functions of temperature and density. In appendix A, we examine the effect of this approximation and show that it leads to errors in the convective flux no larger than 10–20% for the calculations we have done. Since this uncertainty is less than that introduced by other aspects of the modelling, such as different prescriptions for the third order moments (see Fig. 5 of Kupka 2003, for the case of A-stars), we are justified in neglecting this effect in the present analysis. In addition, we show that in the future the correction terms arising from relaxing this assumption can be naturally included within the Reynolds stress formalism.

[2] We note that in our subsequent implementation of the Reynolds stress equations that we *do* use the actual values of c_P and other thermodynamic quantities computed using the OPAL equation of state.

6 COMPARISON WITH PULSATION DATA

For pulsations in the DA and DB stars, we are in the fortunate regime in which the convective turnover time is quite short ($\sim$1 s) compared to the periods of the observed modes ($\sim$100 s). This means that the convection zone responds to the pulsations in a quasi-static manner, so the only input needed for the pulsation calculations is a sequence of static convection zones computed for different effective temperatures. Thus, true time-dependent solutions for the convective region are not needed, which simplifies the modelling considerably.

It has recently been shown (Brickhill 1991a,b; Goldreich & Wu 1999) that the convection zone plays a vital role in the driving of pulsations in the DAV stars, and this is likely to be true of the DBV stars as well. Thus, the observed blue edge and red edge of the instability strip (see Bergeron et al. 1995, 2003) should contain information concerning the dependence of the convective efficiency on $T_{\rm eff}$ and $\log g$.

In addition, the observed nonlinearities in the lightcurves of the DAV's are also believed to be due to the interaction of the convection zone with the pulsations (Wu 2001; Ising & Koester 2001), so it should again be possible to use the observations to constrain different models of convection; this work is presently under way (Montgomery, in preparation). Thus, the pulsating white dwarfs (both DAV's and DBV's) offer a great deal of promise for learning about the physics of convection.

7 CONCLUSIONS

Using a fully non-local model of convection together with a realistic equation of state and opacities, we have calculated envelope models for stellar parameters appropriate for DA and DB white dwarfs. We find good agreement between our models and those obtained through fitting white dwarf spectra, as well as good agreement with the results of hydrodynamic simulations.

First, the maximum convective fluxes in our DA models compare reasonably well with those found in 2D hydrodynamical simulations (Freytag 1995). This result appears more impressive when taking into account that a similar agreement was found for the case of A-stars (Kupka & Montgomery 2002) while MLT type models such as ML1 require a change of the scale length parameter α

by a factor of 4 (see already Freytag 1995). On the other hand, the convective velocities (both vertical and horizontal) differ from each other by a fairly significant amount. At present we do not know whether this signals an incompleteness in the Reynolds stress model or a limitation of the 2D simulations, or both. However, while our rms velocities and those of Freytag (1995) are found to differ by up to a factor of two in the convection zone, we emphasise the completely different results obtained when using a local convection model such as ML1 or ML2. Among other shortcomings, the latter underestimate the size of the convectively mixed region by a factor of at least 10 in terms of mass relative to our new results and even more when compared to those of Freytag (1995). Thus, while the predicted rms velocities at least qualitatively agree when comparing the Reynolds stress formalism applied in this paper with 2D numerical simulations, results from local convection models such as MLT are fundamentally different from the two.

Second, given the widespread use of MLT in stellar and atmospheric modelling, we have compared aspects of our models to MLT models. We find for our DA models that their photospheric temperature structure is best approximated by local MLT models (ML2) having α between ~ 0.7 and ~ 0.9. This is in agreement with the results of Bergeron et al. (1995), who found that their model spectra matched both the optical and UV data best for ML2/α=0.6; for fitting the optical data alone, ML2/α=1.0 also provided a good fit to their observations. Going beyond such fits, our non-local model offers the promise of a unified model for self-consistently computing the velocity field ('microturbulence') which is also required for such model atmosphere fits, something which local models fail to do.

Since the onset of convection goes hand in hand with the onset of pulsation in both the DA's and DB's, we have the opportunity to use asteroseismology to sample their interior structure. First of all, the dependence of the blue edge of the instability strip on $T_{\rm eff}$ and $\log g$ very likely depends on how the convective efficiency varies with these parameters, so the observed blue edge can be used to constrain theories of convection. In addition, recent calculations have shown that the convection zones in these stars may be the main source of the observed non-linearities in their lightcurves (Brickhill 1992a; Wu 2001; Ising & Koester 2001), so it may be possible to use the pulsations themselves to probe the structure of the convection zone. In particular, from observations of a given pulsating star it may be possible to infer the depth of the convection zone as a function of the instantaneous effective temperature (Montgomery, in preparation). This would provide important data for the current convection models.

From an astrophysical standpoint, white dwarf stars are crucial for our understanding of the initial-final mass relation for stars as well as providing an independent method for determining stellar and Galactic ages. In addition, through asteroseismology, they can serve as test beds for nuclear reaction rates (Metcalfe 2003), chemical diffusion (Montgomery et al. 2001), crystallisation (Winget et al. 1997; Montgomery & Winget 1999), and neutrino emission (O'Brien et al. 1998). In order to make maximum use of these inferences, however, model atmospheres need to be applied to the observations of individual white dwarfs in order to derive the stellar parameters (M_*, $T_{\rm eff}$); depending upon the prescription which is adopted for convection, these parameters can vary significantly (e.g. Bergeron et al. 1995). Thus, understanding convection in the context of these stars is vital.

Except for a possible application to RR Lyr stars and Cepheids, the results reported here and in Kupka & Montgomery (2002) represent the limits of what we can treat using our present semi-implicit solver. We are currently in the process of developing a fully-implicit solver, which will allow us to treat thicker convection zones having larger thermal timescales, and, hence, lower effective temperatures. In addition to allowing us to compute cooler models with deeper convection zones for the DA and DB white dwarfs, and the A and F-stars, we would eventually like to study the convection zone of the Sun. This would be an excellent test of the model since a wealth of high-quality data already exists for the solar convection zone. On the same basis, calculations of mixing and overshooting in stellar convective cores may be an even more important application. While the quality of data for probing the effects of convective core overshooting cannot match some of the solar observational results, there are no extra complications as introduced by the large temperature fluctuations and non-grey radiative transfer near the solar surface, which are unaccounted for by the present model but are expected to alter basic quantities such as the derived depth of the solar convection zone. The current accuracy of evolution models of intermediate and high mass stars is still most severely limited by the coarse treatment of convective heat transfer and mixing. At least part of the solution to this problem might be achieved by using a model similar to the one applied in this paper.

ACKNOWLEDGMENTS

We thank Dr. B. Freytag for providing us with results from his simulations and for stimulating discussions, and we also thank Prof. V. Canuto for his insightful comments on our work. This research was supported by the UK Particle Physics and Astronomy Research Council through grants PPA/G/O/2002/00498 and PPA/G/O/1998/00576.

REFERENCES

Asplund M., Ludwig H.-G., Nordlund Å., Stein R. F., 2000, A&A, 359, 669
Beauchamp A., Wesemael F., Bergeron P., Fontaine G., Saffer R. A., Liebert J., Brassard P., 1999, ApJ, 516, 887
Bergeron P., Fontaine G., Billeres M., Boudreault S., Green E. M., 2003, ApJ, in press (astro-ph/0309483)
Bergeron P., Wesemael F., Lamontagne R., Fontaine G., Saffer R. A., Allard N. F., 1995, ApJ, 449, 258
Böhm K. H., Cassinelli J., 1971, A&A, 12, 21
Böhm-Vitense E., 1958, Zeitschrift für Astrophysik, 46, 108
Brickhill A. J., 1991a, MNRAS, 251, 673
Brickhill A. J., 1991b, MNRAS, 252, 334
Brickhill A. J., 1992a, MNRAS, 259, 519
Brickhill A. J., 1992b, MNRAS, 259, 529
Canuto V. M., 1992, ApJ, 392, 218
Canuto V. M., 1993, ApJ, 416, 331
Canuto V. M., 1997, ApJ, 482, 827
Canuto V. M., Dubovikov M., 1998, ApJ, 493, 834
Canuto V. M., Cheng Y., Howard A., 2001, J. Atm. Sci., 58, 1169
Freytag B., 1995, PhD thesis, University of Kiel
Freytag B., Ludwig H.-G., Steffen M., 1996, A&A, 313, 497
Goldreich P., Wu Y., 1999, ApJ, 511, 904
Gryanik, V. M., Hartmann, J., 2002, J. Atm. Sci., 59, 2729
Iglesias C. A., Rogers F. J., 1996, ApJ, 464, 943
Ising J., Koester D., 2001, A&A, 374, 116
Kim Y., Chan K. L., 1998, ApJ, 496, L121

Koester D., Allard N. F., Vauclair G., 1994, A&A, 291, L9
Kupka F., 1999, ApJ, 526, L45
Kupka F., 2003, in Piskunov N. E., Weiss W. W., Gray D. F., eds, IAU Symposium 210: Modelling of Stellar Atmospheres. ASP, San Francisco, in press
Kupka F., Montgomery M. H., 2002, MNRAS, 330, L6
Landstreet J. D., 1998, A&A, 338, 1041
Ludwig H., Freytag B., Steffen M., 1999, A&A, 346, 111
Ludwig H.-G., 2003, in Piskunov N. E., Weiss W. W., Gray D. F., eds, IAU Symposium 210: Modelling of Stellar Atmospheres. ASP, San Francisco, in press (astro-ph/0208583)
Ludwig H.-G., Jordan S., Steffen M., 1994, A&A, 284, 105
Metcalfe T. S., 2003, ApJ, 587, L43
Montgomery M. H., Metcalfe T. S., Winget D. E., 2001, ApJ, 548, L53
Montgomery M. H., Winget D. E., 1999, ApJ, 526, 976
O'Brien M. S., et al., 1998, ApJ, 495, 458
Rast M. P., Nordlund Å, Stein R. F., Toomre J., 1993, ApJ, 408, 53
Rogers F. J., Swenson F. J., Iglesias C. A., 1996, ApJ, 456, 902
Stein R. F., Nordlund Å., 1998, ApJ, 499, 914
Tassoul M., Fontaine G., Winget D. E., 1990, ApJS, 72, 335
Weidemann V., 2000, A&A, 363, 647
Winget D. E., 1982, PhD thesis, University of Rochester
Winget D. E., 1998, Journal of Physics: Condensed Matter, 10, 11247
Winget D. E., Hansen C. J., Liebert J., Van Horn H. M., Fontaine G., Nather R. E., Kepler S. O., Lamb D. Q., 1987, ApJ, 315, L77
Winget D. E., Kepler S. O., Kanaan A., Montgomery M. H., Giovannini O., 1997, ApJ, 487, L191
Winget D. E., van Horn H. M., Tassoul M., Fontaine G., Hansen C. J., Carroll B. W., 1982, ApJ, 252, L65
Wood M. A., 1992, ApJ, 386, 539
Wu Y., 1997, PhD thesis, California Institute of Technology
Wu Y., 2001, MNRAS, 323, 248
Zahn J.-P., 1991, A&A, 252, 179

APPENDIX A: ESTIMATE OF ERRORS ARISING FROM THE IDEAL GAS ASSUMPTION

In this appendix, we give an assessment of the uncertainties introduced by the ideal gas assumption in the Reynolds stress model formalism of Canuto & Dubovikov (1998) we mentioned in Section 5. Essentially, this has meant that the specific heats, c_P and c_V, were treated as constants when computing ensemble averages. To partially correct for this, we have used a realistic equation of state to compute the values of c_P and c_V as functions of ρ and T where they occur in the relevant equations. However, we are necessarily missing any cross terms (moments) that may have arisen when they were averaged against other fluctuating quantities to derive the moment equations themselves.

To provide an estimate of the errors which this may introduce, we consider the convective flux, which is actually the flux of enthalpy, h. From Canuto (1997), equation (19b), we have

$$F_j^C = \overline{\rho h u_j},$$

which, in the absence of a mean flow, we approximate as

$$F_j^C = \overline{\rho}\,\overline{h' u_j'}, \tag{A1}$$

in the Boussinesq sense. Here, u_j is the j-th component of the turbulent velocity, and the overbar denotes an ensemble average. In the present context, we do not consider density-weighted averages, which are more convenient when dealing with a fully compressible flow. In what follows, all variables have been separated into an average and a fluctuating component with respect to ensemble averages. For example, if X represents a given fluctuating quantity (e.g. temperature, velocity, etc.), we write

$$X = \overline{X} + X', \tag{A2}$$

where

$$\overline{X'} = 0. \tag{A3}$$

In the work of Canuto (Canuto 1997; Canuto & Dubovikov 1998) the assumption has been made that the gas is ideal, specifically that $h = c_P T$, with c_P being constant. Here, we consider h to be a function of T and P, i.e., $h = h(T,P)$. If we assume that $T' \ll \overline{T}$, $P' \ll \overline{P}$, we have

$$\begin{aligned} h &= h(\overline{T}+T', \overline{P}+P') && \text{(A4)}\\ &= h(\overline{T},\overline{P}) + h_T\,T' + h_P\,P' + \frac{1}{2}h_{TT}\,T'^2 + O(T'P', P'^2), && \text{(A5)} \end{aligned}$$

where

$$\begin{aligned} h_T &\equiv \left(\tfrac{\partial h}{\partial T}\right)_P &&= c_p\\ h_P &\equiv \left(\tfrac{\partial h}{\partial P}\right)_T &&= (1-\nu_T)/\rho\\ h_{TT} &\equiv \left(\tfrac{\partial^2 h}{\partial T^2}\right)_P &&= \left(\tfrac{\partial c_p}{\partial T}\right)_\rho - \tfrac{\rho\nu_T}{T}\left(\tfrac{\partial c_p}{\partial \rho}\right)_T, \end{aligned}$$

and

$$\nu_T \equiv \frac{\chi_T}{\chi_\rho} = -\left(\frac{\partial \ln\rho}{\partial \ln T}\right)_P,$$

and each of the quantities $h_T, h_P, h_{TT}, c_p, \nu_T$ is evaluated at $\overline{T},\overline{P},\overline{\rho}$ both here and in what follows. Since in the ideal gas case the first order temperature term is already present, and since we wish to go one order beyond this in the temperature and pressure fluctuations, we take the expansion to second order in temperature and first order in pressure. As we will see later, the first-order pressure corrections and the second-order temperature corrections are indeed of similar magnitude.

Taking the ensemble average of equation (A5), we find that

$$\overline{h} = h(\overline{T},\overline{P}) + \frac{1}{2}h_{TT}\overline{T'^2}.$$

Using $h' = h - \overline{h}$, we can substitute the above result into equation (A1) for the convective flux. Writing w and θ for the turbulent velocity and temperature perturbations, (i.e., $\theta \equiv T'$, $w \equiv u_j$), we find that

$$F_C = \overline{\rho}h_T\,\overline{w\theta} + \overline{\rho}h_P\,\overline{wP'} + \frac{1}{2}\overline{\rho}h_{TT}\,\overline{w(\theta^2 - \overline{\theta^2})} + \ldots$$

Since $h_T = c_P$, the first term is the zeroth order term which we have been calling the convective flux, and the other terms are the corrections to it. Let us denote these terms by

$$\begin{aligned} F_0 &= \overline{\rho}c_p\,\overline{w\theta}\\ F_1 &= \overline{\rho}h_P\,\overline{wP'}\\ F_2 &= \frac{1}{2}\overline{\rho}h_{TT}\,\overline{w(\theta^2-\overline{\theta^2})}\\ &= \frac{1}{2}\overline{\rho}h_{TT}\,\overline{w\theta^2}. && \text{(A6)} \end{aligned}$$

The quantity $\overline{wP'}$ is not directly calculated in the present version of the code, although it may be approximated by closures such as those found in Canuto (1992, 1997). For our present purposes, we use the relation

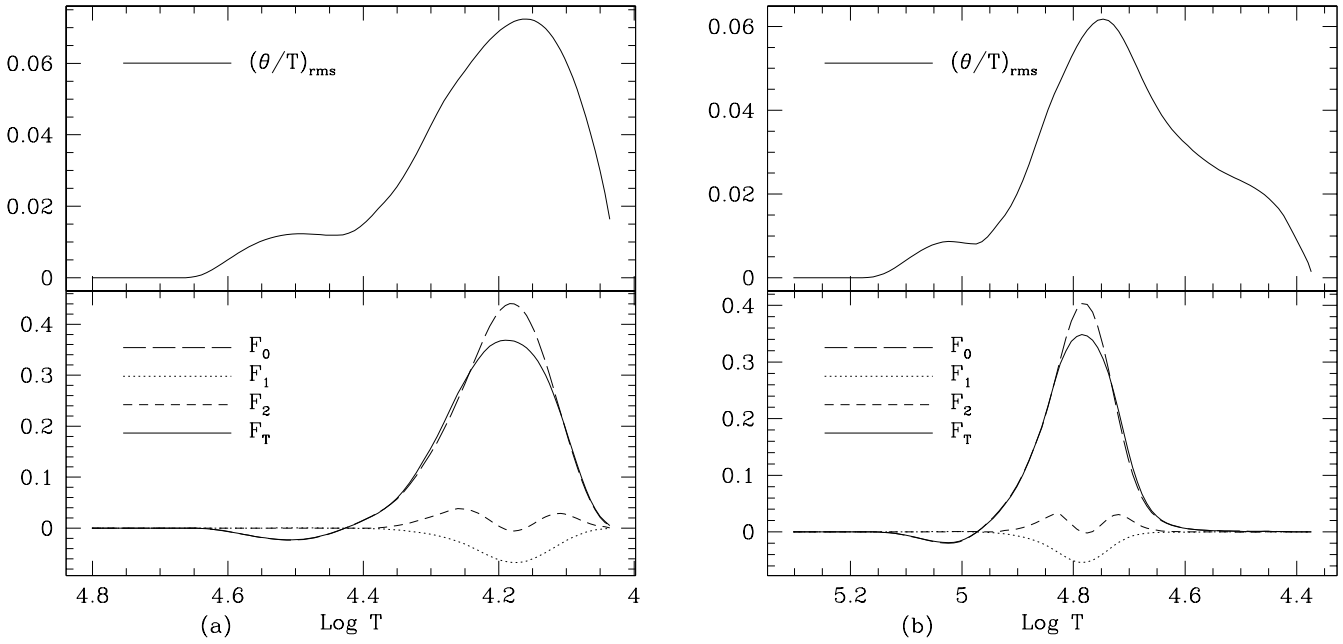

Figure A1. The rms fractional temperature fluctuation (upper panel) and the convective fluxes (lower panel) for a $T_{\rm eff}$=12200 K DA model (a) and a $T_{\rm eff}$=28,000 K DB model (b). The fluxes shown in the lower panel are those given in equation (A6), with the sum of these, $F_{\rm T}$, indicated by the solid curve.

$$P' = \left(\frac{\partial P}{\partial T}\right)_\rho T' = \left(\frac{\partial P}{\partial T}\right)_\rho \theta,$$

to recast $\overline{wP'}$ in terms of $\overline{w\theta}$, which would be exact in the incompressible limit.

In Fig. A1, we examine the relative sizes of these terms for two different white dwarf models: a 12,200 K DA model (a) and a 28,000 K DB model (b). In the upper panels we show the rms fractional temperature fluctuations as taken from our converged nonlocal models; we note that these fluctuations are everywhere less than 8%, justifying our treatment of them as small perturbations. In the lower panel, we plot the leading order flux, F_0 (long-dashed curve), the first order pressure correction to it, F_1 (dotted curve), the second order temperature correction, F_2 (short dashed curve), and the sum of all of these, $F_{\rm T}$ (solid curve). We see that while these correction terms are non-negligible, they would lead to fractional corrections to F_0 of only about 15%. In addition, these corrections appear to be large only in the central part of the convection zone; outside of this region, the convective (enthalpy) flux is essentially given by F_0.

Finally, in Fig. A2, we make a similar plot for an A-star model ($T_{\rm eff}$=7200 K, $\log g$ = 4.4) from our previous paper (Kupka & Montgomery 2002). In contrast to the white dwarf case, we see that there are two different convectively unstable regions, corresponding to He II ionisation ($\log T \sim 4.7$) and H I ionisation ($\log T \sim 4.1$). In the deeper He II zone, we see that these correction terms are negligible. In the H I zone, these terms are larger, driven by the fairly large temperature fluctuations of up to $\sim$ 18%. We see that the main effect is to shift the maximum of the convective flux slightly outward and to decrease its magnitude; even so, this decrease in the maximum convective flux is only about 10%. As in the white dwarf case, we see that these corrections are only significant within the formal convection zone and not in the overshooting regions.

We note that for both Figs. A1 and A2 the models have not been reiterated, i.e., the converged model does not include the corrections to F_0. However, as the difference between F_0 and $F_{\rm T}$ is no more than 15% and as there is a negative feedback, the figures are sufficient to demonstrate the size of the effect. Self-consistent models for the cases shown in Fig. A1 which are based on the full equation (A6) for $F_{\rm T}$ are expected to have a larger convective driving and thus a maximum in $F_{\rm T}$ larger than the one plotted, though still smaller than F_0. The case shown in Fig. A2 is not quite so simple, but a self-consistent solution can be expected to yield a flux which lies between F_T and F_0, regardless of which one is larger.

The additional correction terms which we have derived above (i.e., those in equation A6) pose no problem for the Reynolds stress approach since these new terms involve moments which are already calculated in the current formalism ($\overline{w\theta}, \overline{w\theta^2}$ in the current paper, and eventually $\overline{wP'}$). Thus, even if it turns out that these terms are more important for thicker/cooler convection zones, it should not prevent us from extending the Reynolds stress approach further into this regime.

Finally, we note that the magnitude of the uncertainties in equation (A5) is of order $\sim$ 10%, which is actually less than that introduced by other aspects of the modelling, such as different prescriptions for the third order moments (see Fig. 5 of Kupka 2003, for the case of A-stars). Thus, in the present analysis we are justified in neglecting this effect.

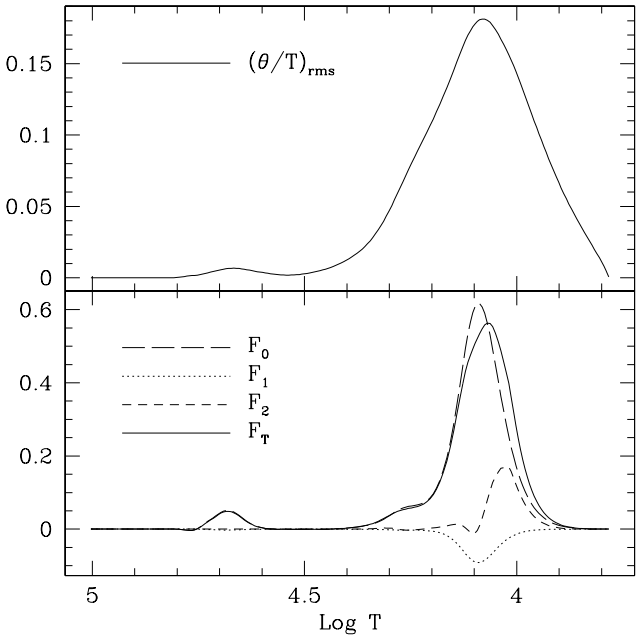

Figure A2. Same as Fig. A1 but for an A-star model having $T_{\rm eff}$=7200 K and $\log g$ = 4.4.